JACS
JOURNAL OF THE AMERICAN CHEMICAL SOCIETY

Article

pubs.acs.org/JACS

Colloidal Atomic Layer Deposition (c-ALD) using Self-Limiting Reactions at Nanocrystal Surface Coupled to Phase Transfer between Polar and Nonpolar Media

Sandrine Ithurria[†] and Dmitri V. Talapin*[,†,‡]

[†]Department of Chemistry and James Frank Institute, University of Chicago, Chicago, Illinois 60637, United States

[‡]Center for Nanoscale Materials, Argonne National Laboratory, Argonne, Illinois 60439, United States

Supporting Information

ABSTRACT: Atomic layer deposition (ALD) is widely used for gas-phase deposition of high-quality dielectric, semiconducting, or metallic films on various substrates. In this contribution we propose the concept of colloidal ALD (c-ALD) for synthesis of colloidal nanostructures. During the c-ALD process, either nanoparticles or molecular precursors are sequentially transferred between polar and nonpolar phases to prevent accumulation of unreacted precursors and byproducts in the reaction mixture. We show that binding of inorganic ligands (e.g., S^{2-}) to the nanocrystal surface can be used as a half-reaction in c-ALD process. The utility of this approach has been demonstrated by growing CdS layers on colloidal CdSe nanocrystals, nanoplatelets, and CdS nanorods. The CdS/CdSe/CdS nanoplatelets represent a new example of colloidal nanoheterostructures with mixed confinement regimes for electrons and holes. In these materials holes are confined to a thin (~1.8 nm) two-dimensional CdSe quantum well, while the electron confinement can be gradually relaxed in all three dimensions by growing epitaxial CdS layers on both sides of the quantum well. The relaxation of the electron confinement energy caused a shift of the emission band from 510 to 665 nm with unusually small inhomogeneous broadening of the emission spectra.

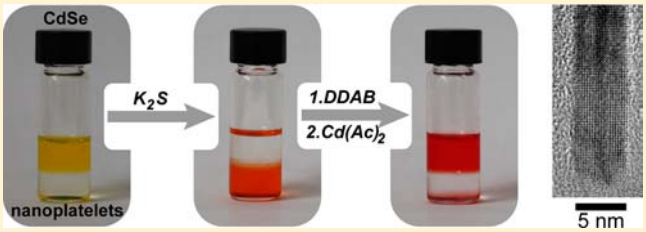

1. INTRODUCTION

Atomic layer deposition (ALD) is a powerful technique for deposition of high-quality thin films of dielectric oxides (e.g., Al_2O_3, HfO_2, etc), semiconductors (ZnO, ZnS, InGaAs), and metals (Pt, Ir, etc) on various substrates.[1,2] Compared to other gas-phase deposition techniques, ALD enables precise control over the layer thickness on the atomic scale and allows conformal deposition on porous and high-aspect ratio substrates. Most ALD processes rely on binary reaction sequences where two surface half-reactions are used to deposit a binary compound.[1,2] Self-limiting surface reactions deliver gaseous precursors to all available surface sites but prevent material deposition beyond single atomic layer.

In this work we discuss the concept of ALD in application to colloidal nanomaterials. The syntheses of functional nanostructures typically involve growth of new inorganic phase at the surface of colloidal "cores".[3] For example, the growth of a wide-gap shell around a semiconductor nanocrystal (NC) is routinely used to obtain core-shells with high quantum efficiency and stability.[4] The growth of an epitaxial shell requires careful control over reactivity and concentrations of the shell precursors and the reaction temperature. If these requirements are not met, then the shell material can nucleate in form of separate nanoparticles (so-called secondary nucleation).[5,6] Secondary nucleation can be significantly suppressed by employing successive ionic layer adsorption and reaction (SILAR) technique that uses successive additions of metal and chalcogen precursors to grow shells of II–VI semiconductors in a layer-by-layer fashion.[7]

SILAR is conceptually related to ALD, but there is an important difference between these techniques. In SILAR no free precursors are allowed to be present after the completion of half-reaction. The amounts of the precursors used for each half-reaction are calculated to match one monolayer coverage for all cores.[6,7] This requires precise knowledge of the total surface area for all cores present in the reaction mixture, which is a very challenging requirement, especially in the case of polydisperse or nonspherical cores. Moreover, SILAR assumes quantitative reaction yields for both half-reactions. Any inaccuracies in estimations of the above parameters accumulate with each SILAR cycle and lead to the lack of control.[5] On the other hand, in traditional gas-phase ALD, precursors are efficiently separated throughout the deposition process by pulsing a purge gas after each half-reaction to remove excess precursor from the chamber. The ALD of a binary compound AB requires a four step sequence: (i) deposition of A layer; (ii) purge to remove all unreacted precursors for A; (iii) deposition of B layer that reacts with A on the surface; and (iv) purge of B precursors before staring new cycle.[1] Steps (i) and (iii) are self-

Received: August 17, 2012
Published: October 12, 2012

   dx.doi.org/10.1021/ja308088d | J. Am. Chem. Soc. 2012, 134, 18585–18590

limiting, once all the surface sites have reacted. Excessive reagents are purged off to prevent their reaction with the following reagent. The purge stages (ii) and (iv) permit using an excess of precursor in each half-cycle to drive saturation of surface binding sites. To design similar processes in a colloidal solution (further referred to as colloidal ALD or c-ALD), a similar sequence of steps should be realized in a liquid phase without compromising colloidal stability of NCs.

We propose a c-ALD process based on self-limiting half-reactions coupled to the phase transfer of NCs or molecular precursors between immiscible nonpolar and polar phases. The phase transfer allows facile removal of unreacted molecular precursors and prevents accumulation of the reaction by-products. During the past decade, colloidal syntheses of high-quality nanomaterials have been dominated by the use of nonpolar solvents and long-chain hydrocarbon ligands sterically stabilizing NCs in nonpolar media.[8] Our approach builds upon recent progress in stabilization of colloidal nanomaterials in highly polar solvents such as formamide (FA), *N*-methyl-formamide (NMF), hydrazine, etc using inorganic ligands, such as S^{2-}, Se^{2-}, $Sn_2S_6^{4-}$, etc.[9−11] We show that the combination of these new surface ligands with traditional approach significantly expands the synthetic toolbox for colloidal nanomaterials.

2. EXPERIMENTAL DETAILS

Nanomaterials Synthesis. CdSe nanocrystals with wurtzite (W-CdSe) and zinc blende (ZB-CdSe) phase, CdS nanorods (NRs), and CdSe nanoplatelets (NPLs) were synthesized following established protocols as described in Supporting Information (SI).

c-ALD by Phase Transfer of Nanoparticles (e.g., NRs). *Method A.* In a 6 mL vial, 1 mL of FA, 2 μL of 40% aqueous solution $(NH_4)_2S$, 1 mL toluene, and 200 μL of CdS NRs dissolved in toluene (20 mg/mL) (or CdSe NCs) were stirred until complete phase transfer of NRs from toluene to FA. The NCs were then moved back to the toluene phase (1 mL) by adding 15 μL of 0.1 M solution didodecyldimethylammonium bromide (DDAB) in toluene and 30 μL of 0.1 M solution tetraethylammonium bromide (Et_4NBr) in formamide. The transfer of NRs from polar to nonpolar phase occurred within 1−2 min (solution was agitated by shaking on a vortex mixer). The addition of Et_4NBr was used to increase the ionic strength in the polar phase leading to more efficient transfer of NRs. The nonpolar phase was then rinsed two times with fresh formamide. Then 1 mL of formamide and 30 μL of 0.1 M $Cd(Ac)_2$ solution in formamide were added to the nonpolar phase and stirred for 5 min at room temperature. The polar phase was rinsed two times with fresh formamide. This cycle could be repeated many times without precipitation of NRs. It required ∼20 min to grow one CdS layer, which is the typical time required for the growth of one layer by SILAR with a waiting time of 10 min after each injection.[5] This approach can be successfully applied to spherical CdSe NCs and CdSe NPLs.

c-ALD in Nonpolar Phase without Phase Transfer (e.g., Spherical Nanocrystals). *Method B1.* In a 6 mL vial, 1 mL of FA, 30 μL of 0.1 M K_2S solution in FA [$(NH_4)_2S$ can also be used as sulfide precursor], 1 mL toluene, 60 μL of 0.1 M DDAB solution in toluene, and 200 μL of a solution of 3.8 nm CdSe NCs in toluene (20 mg/mL) were stirred for 5 min at room temperature. CdSe/S^{2-} NCs remained in the toluene phase stabilized with DDA^+ ligands. The nonpolar phase was washed two times with 1 mL of fresh FA by stirring for 1 min each time. Then, 30 μL of 0.1 M $Cd(OA)_2$ solution in toluene was added to the mixture and stirred for 1 min. Finally the NCs were precipitated with ethanol and resuspended in 400 μL of fresh toluene. By repeating the same process, it was possible to grow at least 10 CdS layers. It was also possible to avoid precipitation of NCs by extracting the excess of $Cd(OA)_2$ with addition of methanol and octadecene (ODE).[12] The NCs stayed in ODE phase, while the excess of $Cd(OA)_2$ was transferred to the toluene/methanol mixture. The extraction should be repeated at least two times. It required ∼10 min for growing one CdS layer.

Method B2. In a 6 mL vial, 1 mL FA, 2 μL of 40% aqueous solution $(NH_4)_2S$, 1 mL of toluene, 200 μL of 3.8 nm CdSe NCs in toluene (20 mg/mL), and 15 μL oleylamine (OAm) were combined and stirred at room temperature for 5 min. The NCs stayed in toluene phase stabilized by OAm. The nonpolar phase containing NCs was washed twice with pure formamide. Then 1 mL of formamide and 30 μL of 0.1 M $Cd(Ac)_2$ solution in formamide were added to the polar phase and stirred for 5 min. The NCs stayed in toluene phase stabilized with OAm, while a layer of Cd^{2+} formed on the surface of CdSe/S^{2-} NCs. The nonpolar phase was rinsed two times with fresh formamide. The successive monolayers were grown in the same way, without precipitation of NCs after each monolayer. It required less than 15 min for growing one CdS layer.

c-ALD Growth in Polar Phase (e.g., NPLs). *Method C.* In a 6 mL vial, 1 mL NMF, 2 μL of 40% aqueous solution $(NH_4)_2S$, 1 mL hexane, 200 μL of CdSe NPLs with the absorption maximum at 510 nm dissolved in hexane (20 mg/mL) were stirred until complete phase transfer of NPLs from hexane to NMF. The polar phase containing CdSe NPLs was rinsed two times with hexane, followed by precipitation with acetonitrile and redispersion in fresh NMF. Then 30 μL of 0.1 M $Cd(Ac)_2$ solution in NMF was added, and the mixture was stirred for 30 s. The NPLs were precipitated with toluene and redispersed in NMF. It required <10 min per CdS layer, and we did not notice any loss of NCs due to the washing steps.

3. RESULTS AND DISCUSSION

Transfer of NCs between Polar and Nonpolar Phases (Method A). c-ALD process can rely on sequential phase transfer of NCs between immiscible polar and nonpolar phases as shown in Figure 1a,b. First, a solution of myristate-capped

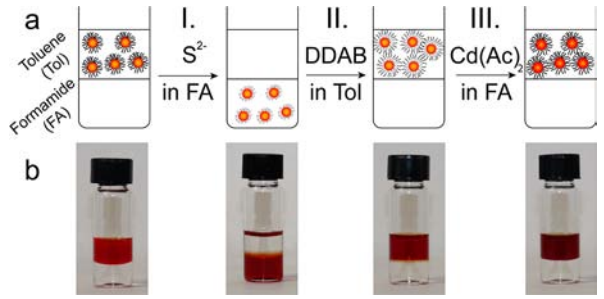

Figure 1. (a) Schematics and (b) photographs showing the sequential growth of one layer of CdS on CdSe nanocrystals. See text for details.

ZB-CdSe NCs dispersed in toluene was exposed to the FA phase containing S^{2-} ions in form of K_2S or $(NH_4)_2S$ (step I in Figure 1a). Nucleophilic S^{2-} ions reacted with electron-deficient Cd^{2+} sites at the NC surface, stripping myristate off and transferring CdSe NCs from toluene to highly polar FA (ε = 108 at 298 K).[9] Negatively charged S^{2-} groups attached to NC surface provided electrostatic stabilization to colloidal CdSe/S^{2-} NCs in FA (Figure 1b) with counterions forming a diffuse layer around each NC.[9,11] The binding of S^{2-} ligands to the NC surface was used as the half-reaction in c-ALD cycle. The upper phase containing organic ligands was discarded, and CdSe/S^{2-} NCs were transferred back into fresh toluene by adding di-*n*-dodecyldimethylammonium bromide (DDAB, step II in Figure 1a). DDA^+ ions formed tight ionic pairs with S^{2-} groups at NC surface and decorated CdSe/S^{2-} NCs with hydrocarbon chains for sterical stabilization in nonpolar solvents.[13] The addition of cadmium acetate (nitrate, perchlorate or oleate can be also used as the cadmium source)

dx.doi.org/10.1021/ja308088d | J. Am. Chem. Soc. 2012, 134, 18585−18590

to fresh FA phase resulted in the growth of Cd^{2+} layer (step III in Figure 1a) which completed the c-ALD cycle.[14]

Synthesis in Nonpolar Phase Coupled to the Transfer of Reagents from the Polar Phase (Methods B1 and B2). Sequential half-reactions can be carried out by transferring either NCs from toluene to FA or S^{2-} and Cd^{2+} from FA phase to toluene while keeping the NCs in nonpolar phase. K_2S and $(NH_4)_2S$ are insoluble in toluene, but DDA^+ ions can assist in the phase transfer of S^{2-} ions by forming DDA_2S ionic pairs.[15] This way S^{2-} can be transferred to toluene to react with NC surface. After the reaction the FA phase was removed, and the toluene phase containing CdSe/S^{2-}/DDA^+ NCs was washed twice with neat FA to extract unreacted DDA_2S.[14] Two extractions with FA were sufficient to remove excess of sulfide ions from the toluene phase. This step would correspond to a purge stage in conventional ALD process. OAm can also be used as the phase-transfer agent for S^{2-} ions instead of DDAB. The addition of $Cd(Ac)_2$ or $CdCl_2$ to the FA phase initiated the second half-reaction in nonpolar phase generating Cd-rich NC surface. Cadmium halides[16] or cadmium acetate[17,18] are insoluble in toluene or hexane, but organic amines can serve as charge-transfer agents through the formation of a complex of the form $Cd(X)_2(amine)_2$, soluble in nonpolar solvents.[18] It was possible to extract excess Cd^{2+} from the nonpolar phase by washing with FA as described for S^{2-}. Two successive extractions were sufficient to remove all unreacted cadmium precursors. The c-ALD cycle was repeated multiple times leading to layer-by-layer growth of CdS shell as shown in Figure 2c,d. All experiments described in this work were carried out at room temperature in air, which made c-ALD process easy to automate using conventional robotic platforms.[18]

Both wurtzite (W) and zinc blende (ZB) CdSe NCs were used as seeds for c-ALD process (Figures 2c,d and S1).[14] In both cases, the growth of CdS shell led to a gradual red shift of the excitonic transitions due to delocalization of the electron wave function into CdS shell (Figure 2a,b) combined with an increase of absorption below ~500 nm corresponding to direct excitation of CdS shell. As expected, the growth of CdS shells resulted in bright photoluminescence of CdSe/CdS NCs; the effect of shell thickness on PL quantum efficiency for ZB-CdSe/CdS and W-CdSe/CdS NCs is shown in Figure S2. TEM images showed an increase of the NC size and no secondary nucleation of CdS particles (Figures 3 and S3). Low-resolution TEM images shown in Figure S3 also confirmed the size and shape uniformity of CdSe/CdS nanostructures prepared by c-ALD process that were comparable to the best reported samples obtained via the SILAR synthesis.[5,6] We did not notice any intraparticle ripening during our c-ALD experiments. We also did not observe losses of NCs at the interface between the polar and the nonpolar phases at each step of the shell growth.

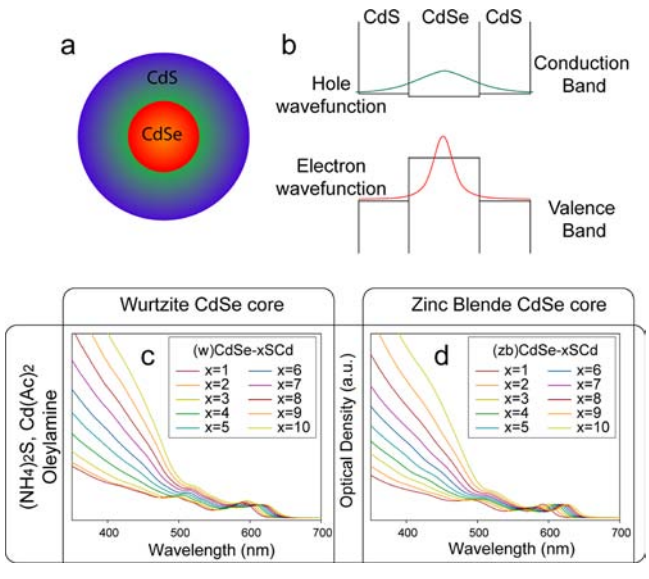

Figure 2. (a) Schematic representation of a CdSe/CdS core−shell nanoheterostructure. (b) The energy level diagram showing the delocalization of electron wave function (green) into CdS shell and the confinement of the hole wave function (red) to CdSe core. (c,d) The absorption spectra of CdSe/CdS nanocrystals measured after 1−10 c-ALD cycles using (c) wurtzite and (d) zinc blende ~3.8 nm CdSe cores.

We studied the parameters affecting uniformity of CdS shell during c-ALD process. In the case of 3.8 nm ZB-CdSe cores, CdS shell could grow either uniformly (Figure 3a) or slightly anisotropically resulting in the core−shells with tetrahedral morphology (Figure 3b). For the isotropic growth, $(NH_4)_2S$ and $Cd(Ac)_2$ were used as the sulfur and cadmium precursors, and OAm was used as the ligand and phase-transfer agent. Primary amines also helped obtaining uniform CdS shells during SILAR process.[5,6] On the other hand, tetrahedral core−shells were obtained when we used $(NH_4)_2S$, $Cd(oleate)_2$, and didodecyldimethylammonium bromide (DDAB). The formation of core−shells with tetrahedral morphology could be explained by the difference in the oleate adsorption energies on the {100} and {111} facets of CdSe/CdS NCs. DFT calculations performed by Li and co-workers showed that the adsorption energy for carboxylate ligands on {111} facets of ZB-CdSe is more than two times larger than the binding energy on {100} facets.[19] Weaker ligand binding should result in the fast growth of {100} facets leading to their disappearance and formation of tetrahedral NCs. We did not notice significant differences in the absorption spectra of CdSe/CdS core−shells with different shell morphology (cf. Figures 2c,d and S4).

Figure 3c,d shows TEM images of CdSe/CdS NCs after 10 c-ALD cycles for 4.1 nm W-CdSe cores. With $(NH_4)_2S$, $Cd(Ac)_2$, and OAm, the core−shell NCs were slightly oblate (Figure 3c), while in presence of DDAB and $Cd(oleate)_2$, the particles appeared more spherical with a tip on one side of the NCs (Figure 3d). Contrary to ZB lattice, the W-CdSe core is noncentrosymmetric, and the (001) facet is structurally different from the (00-1) one.[20] Depending on the ligands and precursors, the reactivity of each facets may vary, leading to various NC shapes.[21,22] For example, phosphonic acids strongly bind to the (100)-type facets of W-CdSe, and the growth of CdS shell occurs preferentially along the [001] direction yielding CdSe/CdS NRs.[23−25]

c-ALD is particularly useful when applied to highly anisotropic cores, such as NPLs and NRs (NRs). For example, we employed this technique to colloidal CdSe NPLs with upper and lower facets represented by the {100} planes of ZB-CdSe phase (Figure S5). The shell growth has been carried out by either transferring NPLs between toluene and FA phases (Method A) or entirely in the polar solvent (NMF) with precipitation steps between the additions of $(NH_4)_2S$ and $Cd(Ac)_2$ (Method C).[14] Figure 4 shows a series of photographs taken during sequential growth of two layers of CdS on CdSe NPLs. The sulfide layer was grown in polar phase, while the cadmium layer was grown in nonpolar phase. We want to

dx.doi.org/10.1021/ja308088d | J. Am. Chem. Soc. 2012, 134, 18585−18590

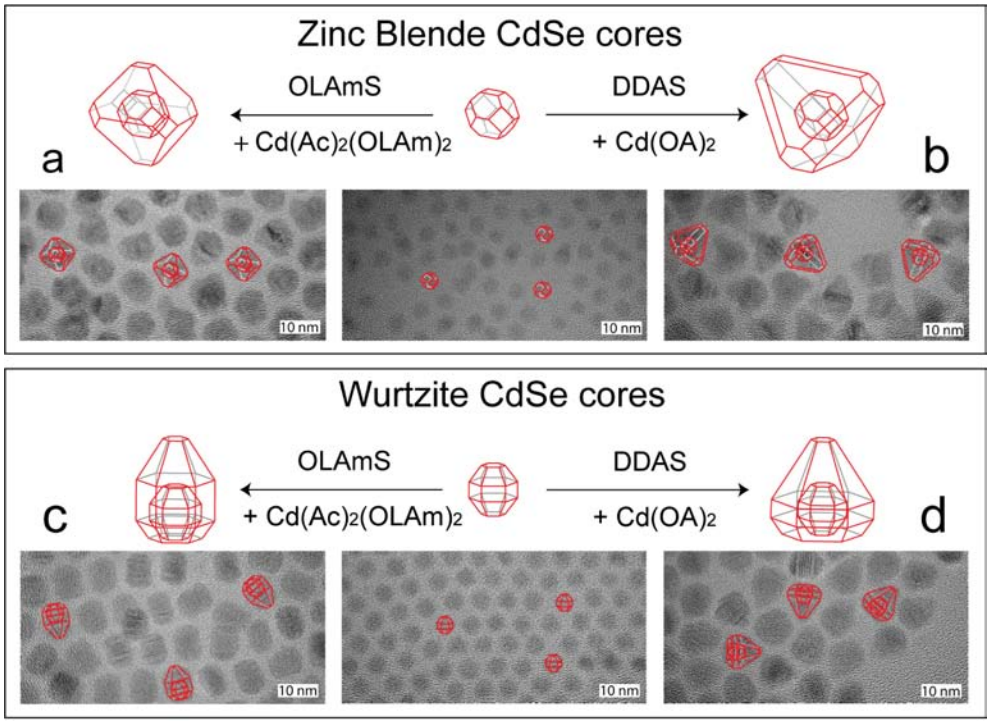

Figure 3. TEM images of CdSe/CdS core shells after 10 c-ALD cycles using spherical CdSe cores with (a,b) zinc blende and (c,d) wurtzite structures. (a,c) CdSe/CdS core−shells synthesized after 10 c-ALD cycles using $(NH_4)_2S$ and cadmium acetate as sulfur and cadmium precursors, respectively, and OAm as the ligand and phase-transfer agent. (b,d) CdSe/CdS core−shells synthesized after 10 c-ALD cycles using $(NH_4)_2S$ and cadmium oleate as sulfur and cadmium precursors, respectively, and DDAB as the phase-transfer agent.

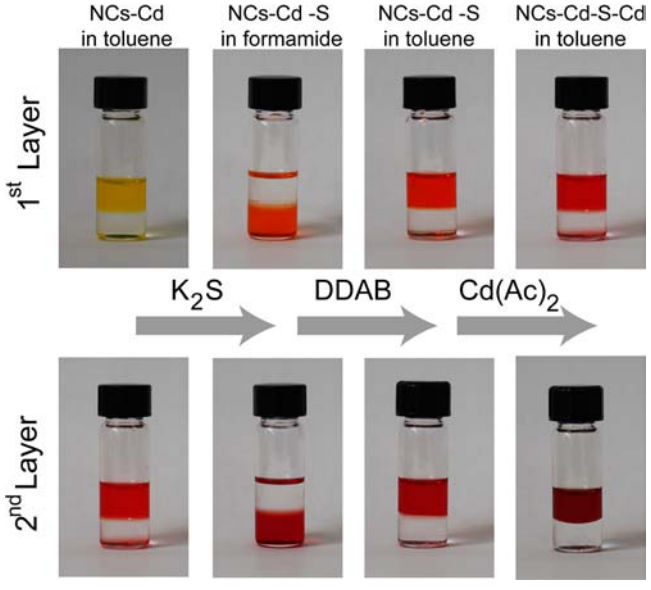

Figure 4. Photographs showing sequential growth of two layers of CdS shell on CdSe NPLs. The addition of K_2S transferred NPLs from nonpolar toluene to polar formamide. The NPLs were transferred back to toluene by addition of DDAB. The excess of DDAB was extracted by washing with formamide, and then the cadmium layer was grown on the surface of CdSe/S^{2-} NPLs surface. The cycle was repeated to add a second layer of CdS (Method A).

emphasize that our attempts to overcoat CdSe NPLs with CdS shell using conventional SILAR approach failed, presumably because of low reactivity of ligand-passivated upper and lower NPL facets.

The electron and hole wave functions in CdSe NPLs are strongly confined along one direction, the thickness. The growth of CdS layer on {001} facets of 1.82 nm thick CdSe NPLs induced a large red shift of the absorption spectra (Figures 4 and 5a), because electrons could easily move between CdSe and CdS parts of the nanostructure.[26,27] The addition of a single CdS layer to both sides of 6-monolayers (1.82 nm) thick CdSe NPLs shifted the first absorption maximum from 510 to 571 nm. Such shift is only slightly smaller than the value predicted by the **k·p** model for 8-monolayers thick CdSe NPLs (576 nm).[28] Along similar lines, the growth of a CdS monolayer on 5-monolayers (1.52 nm) thick CdSe NPLs resulted in the shift of the first excitonic peak from 462 to 544 nm (Figure S6), again only slightly smaller than the value calculated for 7-monolayers thick CdSe NPLs (552 nm).[28] These observations confirm the notion that the majority of the confinement energy in CdSe NPLs comes from electrons that have much smaller (~0.15 m_0) effective mass than holes (~0.5 m_0). These results also suggest that one c-ALD cycle deposited about one unit cell thick layer of CdS. The excitonic peaks further red shifted with increasing the thickness of CdSe shell, thus spanning entire visible range, from 510 nm for bare CdSe NPLs to 665 nm after 7 c-ALD cycles (Figure 5a).

TEM studies of CdSe/CdS NPLs showed that CdS shells uniformly coated CdSe NPLs resulting in the increase of thickness (from 1.8 to 5.9 nm) and lateral dimensions (from ~6 by ~25 nm to ~11 by ~32 nm after 7 c-ALD cycles (Figure 5b,c). Typically, it is difficult to resolve the contrast difference between CdSe and CdS phases in TEM images of spherical CdSe/CdS core−shells or CdSe/CdS dot-in-rod nanostructures. However, the edge view of CdSe/CdS NPLs allowed direct visualization of CdSe core sandwiched between two CdS

dx.doi.org/10.1021/ja308088d | J. Am. Chem. Soc. 2012, 134, 18585−18590

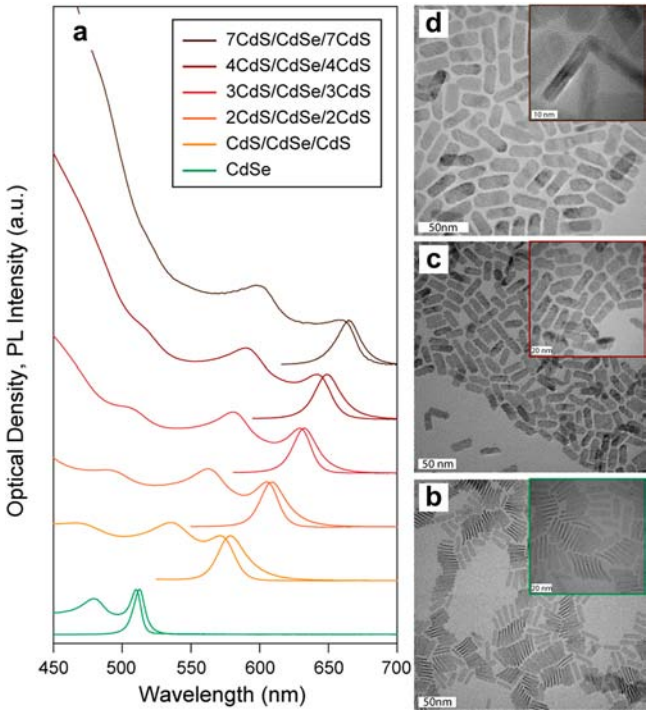

Figure 5. (a) Absorption and emission spectra of *x*CdS/CdSe/*x*CdS NPLs for $x = 0-4$, and 7. CdSe NPLs were dispersed in hexane, while the spectra of core–shell samples spectra have been measured in *N*-methylformamide. All spectra have been normalized to the first excitonic peak and the maximum of the emission peak. (b–d) TEM images of (b) CdSe NPLs, (c) 4CdS/CdSe/4CdS NPLs, and (d) 7CdS/CdSe/7CdS NPLs. The insets in panels (b–d) show closer looks to corresponding samples.

layers (Figures 6a and S7). Counting the numbers of CdS unit cells added to each side of CdSe NPL after seven c-ALD cycles further confirmed the deposition of a single CdS layer per cycle.

The powder X-ray diffraction patterns of CdSe and CdSe/CdS NPLs are shown in Figure 6b. Original CdSe NPLs showed particularly sharp (200) reflection at $2\Theta = 29°$, corresponding to the long NPL axis. The growth of CdS shell resulted in the narrowing of all reflections and their shift to larger 2Θ values due to smaller CdS lattice constant compared to the lattice constant of ZB-CdSe. Strong narrowing of the X-ray reflections could be explained by a good epitaxial relationship between CdSe NPL and CdS shells, leading to a uniform compression of CdSe lattice sandwiched between CdS layers.

CdSe/CdS core–shell NPLs showed strong band edge photoluminescence with quantum efficiency of 20–40%. It should be pointed out that the growth of CdS shell induced some broadening of the PL spectrum. Thus, CdSe NPL cores showed ensemble PL with full width at half-maximum (fwhm) of ~10 nm centered at 510 nm (~48 meV), while the core–shell NPLs with 7-monolayers thick shells showed a PL fwhm ~20 nm centered at 665 nm (~54 meV). Despite this broadening, the core–shell NPLs still showed a significantly narrower ensemble spectra compared to the best spherical CdSe/CdS core–shell and dot-in-rod samples.[6,24] Another interesting feature of CdSe/CdS NPLs was observed in the PL excitation (PLE) spectra recorded at different emission wavelengths. PLE spectroscopy allows optically selecting subpopulations of chromophors that emit at a particular wavelength in an inhomogeneous sample.[29,30] Thus, PLE spectra recorded for conventional NC samples at different emission wavelengths showed different subsets of size-selected NCs (Figure S8a).[30] In contrast, we found that PLE spectra of CdSe/CdS NPLs were totally independent of the emission wavelength (Figure 6c). The same behavior was observed for bare CdSe NPLs (Figure S8b). This observation, when combined with the recent study of single-NPL luminescence,[31] suggests the absence of inhomogeneous broadening in the NPL samples. This, in fact, further supports high uniformity of CdS shells grown by c-ALD technique. The increase of PL fwhm observed for core–shell samples is probably unrelated to inhomogeneous broadening but is an intrinsic effect, either

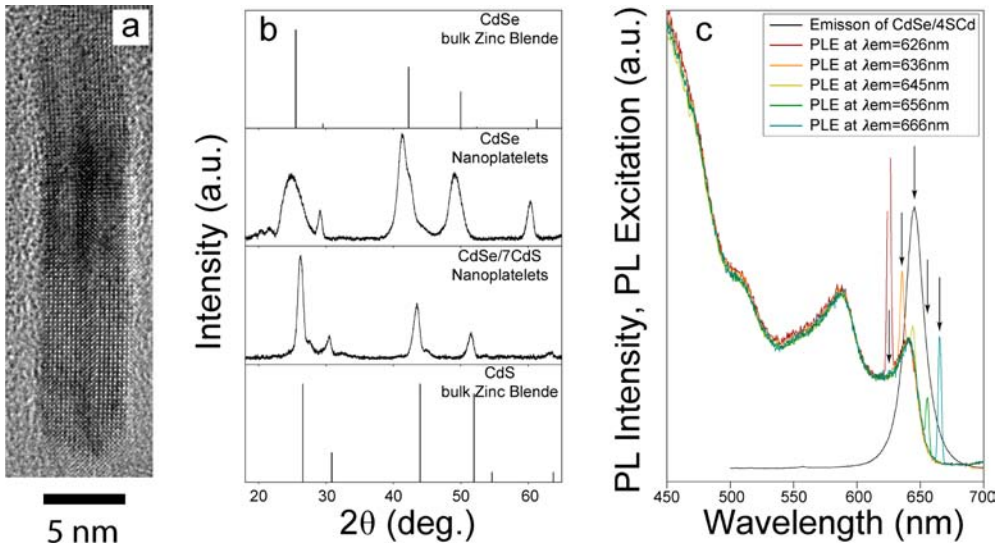

Figure 6. (a) High- resolution TEM image of the edge of CdSe/CdS NPL obtained after seven c-ALD cycles. (b) Powder X-ray diffraction patterns of 6-monolayers (1.82 nm) thick CdSe NPLs and CdS/CdSe/CdS NPLs after 7 c-ALD cycles. (c) Photoluminescence excitation spectra for 4CdS/CdSe/4CdS NPLs recorded for the emission wavelengths 626, 636, 645, 656, and 666 nm. The coincidence of all PLE spectra suggests the absence of inhomogeneous broadening in samples of CdSe/CdS core–shell NPLs.

dx.doi.org/10.1021/ja308088d | J. Am. Chem. Soc. 2012, 134, 18585–18590

related to reduced overlap of the electron and hole wave functions or to local structural defects and surface disorder.

The above examples show that c-ALD is a useful technique that can be applied to various systems. We also applied it to grow a uniform CdS layer on top of 20 nm long and 3.5 nm thick CdS NRs.[14] After 6 c-ALD cycles the diameter of the NRs increased from around 3.5 to around 6 nm (Figure S9). The phosphonic acids used for synthesis of CdS NRs strongly bind to side (100) facets of the NR and lower their reactivity.[8,20] Transferring CdS NRs to a polar solvent by S^{2-} ions allowed us to strip off phosphonate ligands and increase the reactivity of the (100) facets. c-ALD also offers new opportunities for the doping NCs, NRs, and NPLs. The S^{2-} terminated surface can easily react with cationic reagents soluble in FA or NMF, such as $Mn(Ac)_2$, $Pb(Ac)_2$, or $Co(Ac)_2$, allowing incorporation of these ions into the crystal lattice. As an example, Figure S10 shows the absorption and emission spectra of CdS/ZnS NCs[14] doped with Mn^{2+} exhibiting a broad emission band centered at 590 nm typical for the relaxation of tetrahedrally coordinated Mn^{2+} from $^4T_1$ to $^6A_1$ state.[32]

4. CONCLUSION

We have demonstrated colloidal atomic layer deposition of CdS on semiconductor nanomaterials with variable shapes. There are many reasons to believe that the c-ALD approach can be extended to different systems, including materials unstable at high temperatures, such as HgTe. This work also showed the utility of inorganic ligands in colloidal synthesis and opened new opportunities for synthesis of nanoheterostructures with complex compositions and topologies. For example, c-ALD allows precise deposition of a single atomic layer per cycle that can be used for true layer-by-layer design of complex nanoheterostructures.

■ ASSOCIATED CONTENT

Ⓢ Supporting Information

Additional experimental details, figures, and tables. This material is available free of charge via the Internet at http://pubs.acs.org.

■ AUTHOR INFORMATION

Corresponding Author

dvtalapin@uchicago.edu

Notes

The authors declare no competing financial interest.

■ ACKNOWLEDGMENTS

We thank D. Dolzhnikov and J. Huang for help with synthesis of CdSe NPLs and dot-in-rods. We are also very thankful to R. Schaller and A. Nag for fruitful discussions. The work was supported by NSF CAREER under award no. DMR-0847535 and by the University of Chicago and Department of Energy under section H.35 of U.S. DOE contract no. DE.AC02-06CHl1357. D.V.T. also thanks the David and Lucile Packard Foundation. This work used facilities supported by NSF MRSEC Program under award no. DMR-0213745. The work at the Center for Nanoscale Materials (ANL) was supported by the US Department of Energy under contract no. DE-AC02-06CH11357.

■ REFERENCES

(1) George, S. M. *Chem. Rev.* **2010**, *110*, 111−131.
(2) Puurunen, R. L. *J. App. Phys* **2005**, *97*, 121301−52.
(3) Buck, M. R.; Bondi, J. F.; Schaak, R. E. *Nat. Chem.* **2012**, *4*, 37−44.
(4) Reiss, P.; Protière, M.; Li, L. *Small* **2009**, *5*, 154−168.
(5) Ghosh, Y.; Mangum, B. D.; Casson, J. L.; Williams, D. J.; Htoon, H.; Hollingsworth, J. A. *J. Am. Chem. Soc.* **2012**, *134*, 9634−9643.
(6) Greytak, A. B.; Allen, P. M.; Liu, W.; Zhao, J.; Young, E. R.; Popovic, Z.; Walker, B. J.; Nocera, D. G.; Bawendi, M. G. *Chem. Sci.* **2012**, *3*, 2028−2034.
(7) Li, J. J.; Wang, Y. A.; Guo, W.; Keay, J. C.; Mishima, T. D.; Johnson, M. B.; Peng, X. *J. Am. Chem. Soc.* **2003**, *125*, 12567−12575.
(8) Yin, Y.; Alivisatos, A. P. *Nature* **2005**, *437*, 664−670.
(9) Nag, A.; Kovalenko, M. V.; Lee, J.-S.; Liu, W.; Spokoyny, B.; Talapin, D. V. *J. Am. Chem. Soc.* **2011**, *133*, 10612−10620.
(10) Kovalenko, M. V.; Scheele, M.; Talapin, D. V. *Science* **2009**, *324*, 1417−1420.
(11) Kovalenko, M. V.; Bodnarchuk, M. I.; Zaumseil, J.; Lee, J.-S.; Talapin, D. V. *J. Am. Chem. Soc.* **2010**, *132*, 10085−10092.
(12) Yu, W. W.; Qu, L.; Guo, W.; Peng, X. *Chem. Mater.* **2003**, *15*, 2854−2860.
(13) Kovalenko, M. V.; Bodnarchuk, M. I.; Talapin, D. V. *J. Am. Chem. Soc.* **2010**, *132*, 15124−15126.
(14) See Supporting Information for additional details.
(15) Ueda, M.; Oishi, Y.; Sakai, N.; Imai, Y. *Macromolecules* **1982**, *15*, 248−251.
(16) Hines, C. C.; Reichert, W. M.; Griffin, S. T.; Bond, A. H.; Snowwhite, P. E.; Rogers, R. D. *J. Mol. Struct.* **2006**, *796*, 76−85.
(17) Liu, Y.-H.; Wang, F.; Wang, Y.; Gibbons, P. C.; Buhro, W. E. *J. Am. Chem. Soc.* **2011**, *133*, 17005−17013.
(18) Ojo, W.-S.; Xu, S.; Delpech, F.; Nayral, C.; Chaudret, B. *Angew. Chem., Int. Ed.* **2011**, *51*, 738−741.
(19) Liu, L.; Zhuang, Z.; Xie, T.; Wang, Y.-G.; Li, J.; Peng, Q.; Li, Y. *J. Am. Chem. Soc.* **2009**, *131*, 16423−16429.
(20) Manna, L.; Scher, E. C.; Alivisatos, A. P. *J. Am. Chem. Soc.* **2000**, *122*, 12700−12706.
(21) Puzder, A.; Williamson, A. J.; Zaitseva, N.; Galli, G.; Manna, L.; Alivisatos, A. P. *Nano Lett.* **2004**, *4*, 2361−2365.
(22) Rempel, J. Y.; Trout, B. L.; Bawendi, M. G.; Jensen, K. F. *J. Phys. Chem. B* **2006**, *110*, 18007−18016.
(23) Talapin, D. V.; Koeppe, R.; Götzinger, S.; Kornowski, A.; Lupton, J. M.; Rogach, A. L.; Benson, O.; Feldmann, J.; Weller, H. *Nano Lett.* **2003**, *3*, 1677−1681.
(24) Carbone, L.; Nobile, C.; De Giorgi, M.; Sala, F. D.; Morello, G.; Pompa, P.; Hytch, M.; Snoeck, E.; Fiore, A.; Franchini, I. R.; Nadasan, M.; Silvestre, A. F.; Chiodo, L.; Kudera, S.; Cingolani, R.; Krahne, R.; Manna, L. *Nano Lett.* **2007**, *7*, 2942−2950.
(25) Talapin, D. V.; Nelson, J. H.; Shevchenko, E. V.; Aloni, S.; Sadtler, B.; Alivisatos, A. P. *Nano Lett.* **2007**, *7*, 2951−2959.
(26) Peng, X.; Schlamp, M. C.; Kadavanich, A. V.; Alivisatos, A. P. *J. Am. Chem. Soc.* **1997**, *119*, 7019−7029.
(27) Borys, N. J.; Walter, M. J.; Huang, J.; Talapin, D. V.; Lupton, J. M. *Science* **2010**, *330*, 1371−1374.
(28) Ithurria, S.; Tessier, M. D.; Mahler, B.; Lobo, R. P. S. M.; Dubertret, B.; Efros, A. L. *Nat. Mater.* **2011**, *10*, 936−941.
(29) Norris, D. J.; Bawendi, M. G. *Phys. Rev. B* **1996**, *53*, 16338−16346.
(30) Talapin, D. V.; Haubold, S.; Rogach, A. L.; Kornowski, A.; Haase, M.; Weller, H. *J. Phys. Chem. B* **2001**, *105*, 2260−2263.
(31) Tessier, M. D.; Javaux, C.; Maksimovic, I.; Loriette, V.; Dubertret, B. *ACS Nano* **2012**, *6*, 6751−6758.
(32) Pradhan, N.; Sarma, D. D. *J. Phys. Chem. Lett.* **2011**, *2*, 2818−2826.